Overexpression of diacylglycerol kinase eta (DGKη) enhances Gα$_q$-coupled GPCR signaling

Joseph E. Rittiner, Victoria E. Brings, and Mark J. Zylka

Department of Cell Biology and Physiology, UNC Neuroscience Center, University of North Carolina, Chapel Hill, North Carolina

Running title: DGKη regulates GPCR signaling

To whom correspondence should be addressed:

Mark J. Zylka, Department of Cell Biology & Physiology, 5109D NRB, CB #7545

The University of North Carolina at Chapel Hill, Chapel Hill, NC 27599-7545

Tel: 919-966-2540; Fax: 919-966-3870; Email: zylka@med.unc.edu

Text pages: 39

Tables: None

Figures: 7

References: 59

Words in Abstract: 231

Words in Introduction: 420

Words in Discussion: 1,112

Abbreviations:

AUC – area under the curve; BPD – bipolar disorder; DAG – diacylglycerol; DGK –
diacylglycerol kinase; EGFR – epidermal growth factor receptor; GPCR – G protein-coupled
receptor; GRK – G protein-coupled receptor kinase; IP$_3$ – inositol 1,4,5-trisphosphate; PA –
phosphatidic acid; PIP$_2$ – phosphatidylinositol 4,5-bisphosphate; PKC – protein kinase C; PLC –
phospholipase C; PMA – phorbol-12-myristate-13-acetate; SERCA – sarco/endoplasmic
reticulum calcium ATPase; WT – wild-type

ABSTRACT

Multiple genome-wide association studies have linked diacylglycerol kinase eta (DGKη) to bipolar disorder (BPD). Moreover, DGKη expression is increased in tissue from patients with BPD. How increased levels of this lipid kinase might affect cellular functions is currently unclear. Here, we overexpressed mouse DGKη in HEK293 cells to examine substrate specificity and signaling downstream of endogenous G protein-coupled receptors (GPCRs). We found that DGKη can phosphorylate diacylglycerol (DAG) with different acyl side chains (8:0, 12:0, 18:1). In addition, overexpression of DGKη enhanced calcium mobilization after stimulating muscarinic receptors with carbachol and after stimulating purinergic receptors with ATP. This effect required DGKη catalytic activity, as assessed using a kinase-dead (G389D) mutant and multiple truncation constructs. DGKη was localized throughout the cytosol and did not translocate to the plasma membrane after stimulation with carbachol. Since protein kinase C (PKC) can be activated by DAG and promotes receptor desensitization, we also examined functional interactions between PKC and DGKη. We found that acute activation of PKC with phorbol 12-myristate 13-acetate (PMA) shortened carbachol-evoked calcium responses and occluded the effect of overexpressed DGKη. Moreover, inhibition of PKC activity with bisindolylmaleimide I (BIM I) produced the same enhancing effect on carbachol-evoked calcium mobilization as overexpressed DGKη, and overexpression of DGKη produced no additional effect on calcium mobilization in the presence of BIM I. Taken together, our data suggest that DGKη enhances GPCR signaling by reducing PKC activation.

3

INTRODUCTION

Diacylglycerol kinases (DGKs) are a large family of enzymes that catalyze the phosphorylation of the membrane lipid diacylglycerol (DAG) to phosphatidic acid (PA) (van Blitterswijk and Houssa, 2000; Sakane et al., 2007). DAG and PA are important second messengers and regulate diverse proteins and pathways, including protein kinase C (PKC) (Mellor and Parker, 1998), ion channels (Lucas et al., 2003), endocannabinoid production (Gregg et al., 2012), and phosphoinositide synthesis (Jenkins et al., 1994). DGKs are thus well positioned to regulate diverse intracellular signaling pathways (Merida et al., 2008).

In recent years, several studies have identified genetic associations between *DGKH* and bipolar disorder (BPD) (Baum et al., 2008; Squassina et al., 2009; Takata et al., 2011; Weber et al., 2011; Yosifova et al., 2011; Zeng et al., 2011). *DGKH* is the gene that encodes diacylglycerol kinase eta (DGKη). In addition, Moya and colleagues found that DGKη mRNA was expressed at higher levels in post-mortem tissue samples from patients with BPD than unaffected controls (Moya et al., 2010). DGKη is a Type II DGK with two known splice variants (Klauck et al., 1996; Murakami et al., 2003), and was recently implicated in lung cancer (Nakano et al., 2013). However, how alterations in DGKη levels might affect cellular functions or contribute to BPD pathogenesis is currently unknown.

Dysregulation of G protein-coupled receptor (GPCR) activity is involved in the pathology of many psychiatric disorders, including BPD (Catapano and Manji, 2007). Indeed, tissues from BPD patients exhibit changes in GPCR (Pantazopoulos et al., 2004) and G protein subunit (Young et al., 1993; Rao et al., 2009) expression, enhanced receptor-G protein coupling (Friedman and Wang, 1996), and decreased expression of GRK3, a GPCR-regulating kinase (Rao et al., 2009). Furthermore, therapeutic concentrations of lithium and valproate, common

treatments of BPD, inhibit G protein activation after GPCR stimulation in cell membranes

(Avissar et al., 1988) and platelets from bipolar patients (Hahn et al., 2005).

Given that DGKη is expressed at higher levels in BPD patients and has the potential to

affect GPCR signaling, we sought to determine if overexpression of DGKη affected GPCR

signaling in HEK293 cells, a model cell line with well-characterized GPCR signaling cascades

(Luo et al., 2008). Here, we found that overexpression of DGKη dramatically increased the

duration of calcium responses after stimulating endogenous $G\alpha_q$-coupled GPCRs. The effect of

DGKη overexpression was dependent on DGKη catalytic activity and was blocked by inhibition

of PKC. Taken together, our data suggest that DGKη enhances GPCR signaling by attenuating

PKC activity, possibly by attenuating PKC-dependent receptor desensitization.

MATERIALS AND METHODS

Materials

Carbamoylcholine chloride (carbachol), D-sorbitol, n-butanol, ethylenediaminetetraacetic acid (EDTA), phenylmethanesulfonyl fluoride (PMSF), sodium fluoride, DL-dithiothreitol (DTT), sodium deoxycholate, adenosine 5'-triphosphate disodium salt (ATP), HEPES sodium salt, glycerol, sodium pyrophosphate, Dulbecco's phosphate buffered saline (PBS), fatty acid-free bovine serum albumin (BSA), poly-D-lysine, bromophenol blue, and phorbol 12-myristate 13-acetate (PMA) were purchased from Sigma-Aldrich, St. Louis, MO. Concentrated hydrochloric acid, Tris hydrochloride (Tris-HCl), sodium chloride (NaCl), magnesium chloride hexahydrate ($MgCl_2$), sodium dodecyl sulfate (SDS), Triton X-100, Tween 20, and D-glucose were purchased from Fisher Scientific, Waltham, MA. Bisindolylmaleimide I (BIM I) was purchased from Cayman Chemical, Ann Arbor, MI. Gö6976 was purchased from Tocris Bioscience, Bristol, UK. BisNonidet P40 substitute (NP40) was purchased from USB Corporation, Cleveland, OH. [γ-^{32}P]-labeled ATP (6000 Ci/mmol, 150 mCi/ml) was purchased from Perkin Elmer, Waltham, MA.

Molecular Biology

A full-length clone of mouse DGKη isoform 1 was generated by PCR amplification using cDNA from C57BL/6 mouse neurons as a template (bases 1-3471 from GenBank accession #NM_001081336.1) (Murakami et al., 2003). The initial clone was found to be unstable due to high GC content at the 5' end of the DGKη coding sequence. To remedy this problem, the first 69 bases of the DGKη coding sequence were modified to decrease GC content while preserving the wild-type (WT) DGKη amino acid sequence (native sequence: ATG GCC GGG GCC GGC

AGC CAG CAC CAC CCT CAG GGC GTC GCG GGA GGA GCG GTC GCT GGG GCC

AGC GCG; modified sequence: ATG GCA GGA GCA GGA AGT CAG CAT CAT CCT CAG

GGA GTT GCA GGA GGA GCA GTT GCA GGA GCA ACT GCA). The resulting construct

was stable and was used to generate all subsequent constructs. DGKη truncation constructs were

generated by PCR amplification. The G389D point mutant was generated by traditional PCR-

based mutagenesis. Full-length DGKη and all DGKη constructs were inserted into the multiple

cloning site of pcDNA 3.1(+) downstream of monomeric RFP lacking a stop codon, to create

fusion constructs with N-terminal RFP tags. A DGKη-646Δ fusion construct with an N-terminal

Venus tag was generated in the same fashion. All constructs contained a Kozak consensus

sequence and were sequence verified.

Cell Culture

HEK293 cells were grown in Dulbecco's modified Eagle's medium (DMEM; Gibco,

Grand Island, NY) containing 10% fetal bovine serum, 100 U/ml penicillin, and 100 μg/ml

streptomycin at 37°C and 5% CO_2. Cells were plated on polylysine-coated glass-bottom dishes

(MatTek, Ashland, MA) for calcium imaging, polylysine-coated glass coverslips (Brain

Research Laboratories, Waban, MA) for immunostaining, and polylysine-coated 6-well plates

(Corning, Corning, NY) for all other experiments. Twenty-four hours after plating, cells were

transfected with Lipofectamine/Plus (Invitrogen, Carlsbad, CA) in serum-free DMEM according

to the manufacturer's instructions. Each plate/well was transfected with 500 ng of each DNA

construct, and the total amount of DNA per transfection was normalized to 1 μg with empty

vector. After 4 hours, the transfection medium was replaced with fresh growth medium. All

experiments were performed 24 hours after transfection.

Calcium Imaging

Calcium imaging was performed as described previously (Rittiner et al., 2012). Briefly, HEK293 cells expressing various DGKη constructs and controls were washed twice in HBSS assay buffer (Invitrogen; 140 mg/L $CaCl_2$, 100 mg/L $MgCl_2$-$6H_2O$, 100 mg/L $MgSO_4$-$7H_2O$, 400 mg/L KCl, 60 mg/L KH_2PO_4, 350 mg/L $NaHCO_3$, 8 g/L NaCl, 48 mg/L Na_2HPO_4, 1 g/L D-glucose, supplemented with 2.4 g/L HEPES, 2 g/L D-glucose, and 0.1% fatty acid-free BSA, pH 7.3) and loaded with 2 µM Fura-2 AM (Invitrogen) in 0.02% Pluronic F-127 (Invitrogen) in assay buffer for 1 hour at room temperature. For experiments lacking extracellular calcium, identical assay buffer lacking $CaCl_2$ was used throughout the procedure. Cells were then washed three times in assay buffer, incubated at room temperature for 30 minutes, and imaged on an Eclipse Ti microscope (Nikon, Tokyo, Japan) at room temperature. A DG-4 light source (Sutter, Novato, CA), CFI Plan Fluor 20x objective (Nikon), Clara DR-328G-C01-SIL CCD camera (Andor, Belfast, UK), and NIS Elements imaging software (Nikon) were used to image calcium responses. 500-ms excitation at 340 nm and 250-ms excitation at 380 nm was used for all experiments. Fura-2 emission was measured at 510 nm.

Fresh assay buffer was added prior to each experiment. After 40 seconds of baseline imaging, the assay buffer was aspirated and agonist solution was added. All solutions were aspirated and pipetted manually. Aspiration or addition of buffer alone did not cause calcium responses (data not shown, see Fig. 6B PMA-only trace for equivalent experiment). For PKC inhibition experiments, inhibitor was added in assay buffer 30 minutes prior to imaging and was present in all wash and agonist solutions. Only cells that expressed visible RFP fluorescence, had low baseline Fura-2 ratios (< 0.6), and responded to agonist stimulation (Fura-2 ratio > 0.8 at

8

any time after agonist addition) were analyzed. For experiments using cells transfected with

RFP-DGKη-Δ645 and Venus-DGKη-646Δ, only cells expressing both visible RFP fluorescence

and visible Venus fluorescence were analyzed. Real-time response profiles were generated as

described previously (Rittiner et al., 2012). Area under curve (AUC) and peak response values

were calculated relative to baseline Fura-2 ratios on a cell-by-cell basis and averaged over all

cells in each condition. To control for day-to-day variation in calcium responses, control cells

expressing RFP alone were tested as part of each experiment. AUC and peak response values

were then normalized such that RFP alone was set at a value of 1. To create scatter plots

comparing expression and AUC values, RFP-DGKη expression levels were calculated for each

cell by quantifying RFP fluorescence.

Confocal Microscopy

HEK293 cells expressing RFP-DGKη were washed twice in HBSS assay buffer and

imaged using a CSU-10 spinning disc confocal scanner (Yokogawa, Tokyo, Japan) mounted on a

TE2000 microscope (Nikon). An Argon/Krypton laser light source, Orca-ER camera

(Hamamatsu Photonics, Hamamatsu, Japan), and SimplePCI imaging software (Hamamatsu)

were used to image RFP-tagged DGKη. After approximately 1 minute of baseline imaging,

assay buffer was replaced with buffer containing 10 µM carbachol or 500 mM sorbitol, and

imaging continued for an additional 15 minutes. Solutions were removed and added by manual

pipetting.

Immunostaining

HEK293 cells expressing RFP were incubated in PBS alone or 300 nM PMA in PBS for 10 minutes at 37°C then fixed in ice-cold 4% paraformaldehyde (Fisher) for 15 minutes. After incubating in 0.5% Triton X-100 in PBS for 15 minutes, coverslips were blocked for 30 minutes in blocking solution [0.1% Triton X-100 and 5% normal goat serum (Invitrogen) in PBS] then incubated with Rabbit anti-PKCδ primary antibody (Santa Cruz Biotechnology, Santa Cruz, CA) in blocking solution overnight at 4°C. Cells were then washed with 10% goat serum in PBS for 30 minutes and incubated in Alexa Fluor 488-conjugated Goat anti-Rabbit secondary antibody (Invitrogen) and DRAQ5 nuclear dye (Cell Signaling, Beverly, MA) in blocking solution for 1 hour at room temperature. Cells were washed three times (5 minutes/wash) with PBS between each step. Coverslips were mounted onto microscope slides (Fisher) with Fluoro-Gel (Electron Microscopy Sciences, Hatfield, PA) and stored at 4°C. Slides were imaged at room temperature the following day on an LSM 510 microscope (Zeiss, Oberkochen, Germany), using multiline Argon and Helium-Neon laser light sources, a 63x objective, and ZEN imaging software (Zeiss).

In-vitro Kinase Assay

The DGK *in vitro* kinase assay was adapted from previous studies (Kanoh et al., 1992; Ohanian and Heagerty, 1994). HEK293 cells expressing RFP-tagged DGKη (WT or truncation constructs) or RFP alone were washed twice with ice-cold PBS and scraped into ice-cold lysis buffer [50 mM Tris-HCl pH 7.5, 150 mM NaCl, 1 mM EDTA, 1 mM PMSF, 1x Complete Mini protease inhibitor cocktail (Roche, Basel, Switzerland), 1x Phosphatase Inhibitor Cocktail 2 (Sigma), to preserve any potential phosphorylation events on protein]. Cells were disrupted by brief sonication on ice, and debris was collected by centrifugation at 10,000g for 10 minutes at 4°C. Clarified lysates were kept on ice.

10

The final reaction mixture contained 50 mM Tris-HCl pH 7.4, 100 mM NaCl, 20 mM NaF, 10 mM MgCl$_2$, 1 mM DTT, 1 mM EDTA, 1 mM sodium deoxycholate, 0.5 mM DAG (8:0, 12:0, or 18:1), 1 mM [γ-^{32}P]ATP (50 µCi/rxn), and lysate; reaction volume was 50 µl. A calculated amount of 1,2-dioctanoyl-glycerol (8:0 DAG), 1,2-dilauroyl-glycerol (12:0 DAG), or 1,2-dioleoyl-glycerol (18:1 DAG) in chloroform (Avanti Polar Lipids, Alabaster, AL) was deposited in a glass tube under a stream of dry nitrogen gas. The DAG was then resuspended in an appropriate amount of 5x kinase buffer (250 mM Tris-HCl pH 7.4, 500 mM NaCl, 100 mM NaF, 50 mM MgCl$_2$, 5 mM DTT, 5 mM EDTA) and 10 mM sodium deoxycholate by brief bath sonication. 15 µl of the DAG suspension was added to a tube containing 20 µl of water, followed by 5 µl of 10 mM [γ-^{32}P]ATP. The reaction was initiated by adding 10 µl of lysate, incubated for 3 minutes at 30°C, and then stopped by adding 25 µl of 12 N HCl followed by 750 µl of water saturated with n-butanol. Lipids were extracted from the reaction mixture by adding 500 µl of n-butanol, mixing thoroughly, and separating by centrifugation at 1,000g for 5 minutes. 450 µl of the organic phase was washed with 500 µl of n-butanol-saturated water and separated by centrifugation, with care taken not to disturb the aqueous phase. 350 µl of this organic phase was then washed again in the same fashion. Finally, 250 µl of the washed organic phase was transferred to a scintillation vial containing 2 ml of ScintiSafe Econo 2 scintillation fluid (Fisher), mixed gently, and counted on a Wallac Rackbeta 1209 liquid scintillation counter (LKB Instruments, Mount Waverley, Australia).

For experiments comparing different DGKη truncation constructs, each lysate sample was analyzed by anti-RFP western blotting as described below, and the band intensity was quantified using ImageJ image analysis software (National Institutes of Health, Bethesda, MD).

The DGKη activity data were corrected for differences in expression, and normalized such that RFP alone was set at a value of 0, and wild-type DGKη was set at a value of 1.

Western Blotting

A 15 µl portion of each lysate used in the *in vitro* kinase assay was mixed with an appropriate amount of 4x Laemmli sample buffer [125 mM Tris-HCl, 40% (v/v) glycerol, 2% (v/v) SDS, 10% (v/v) β-mercaptoethanol (Bio-Rad, Hercules, CA), 0.02% (w/v) bromophenol blue], and separated by SDS-PAGE on a 4-15% gradient gel (Bio-Rad) at 100 V for 1 hour. Proteins were transferred to a polyvinylidine fluoride (PVDF) membrane (Bio-Rad) at 100 V for 70 minutes on ice, and blocked with 5% nonfat milk (Bio-Rad) in TBST (100 mM Tris-HCl pH 7.5, 165 mM NaCl, 0.1% Tween 20) for 1 hour at room temperature. Blots were then incubated with Rabbit anti-RFP primary antibody (Invitrogen) in 5% BSA (Sigma) in TBST overnight at 4°C. The following day, blots were washed three times (5 minutes/wash) with TBST and incubated with IRDye800-conjugated Donkey anti-Rabbit secondary antibody (LI-COR, Lincoln, NE) in 5% nonfat milk/TBST for 1.5 hours at room temperature. Blots were then washed three times (5 minutes/wash) with TBST and imaged on an Odyssey CLx infrared imaging system (LI-COR).

Co-immunoprecipitation

HEK293 cells expressing tagged DGKη truncation constructs or fluorescent tags alone were washed twice with ice-cold PBS and scraped into ice-cold glycerol-Co-IP buffer containing 50 mM HEPES pH 7.4, 250 mM NaCl, 2 mM EDTA, 10% (v/v) glycerol, 0.5% (v/v) NP40, 1x protease inhibitor cocktail, and 1x phosphatase inhibitor cocktail. Cellular debris was removed

by centrifugation at 10,000g for 10 minutes at 4°C and input aliquots of the clarified lysate were

set aside. The remaining lysate was then incubated with Chicken anti-GFP primary antibody

(Aves Labs, Tigard, OR) or normal Chicken IgY control (Santa Cruz) for 3 hours at 4°C with

gentle mixing. Agarose beads coupled to Goat anti-Chicken IgY (Aves) were then added to each

sample and incubated for 1 hour at 4°C. The beads were washed four times (5 minutes/wash)

with ice-cold glycerol Co-IP buffer, and bound proteins were eluted from the beads by

incubation with 4x Laemmli sample buffer for 15 minutes at 37°C. Input and IP fractions were

then separated by SDS-PAGE, transferred to PVDF membrane, and blotted as described above,

using Rabbit anti-RFP primary antibody. After imaging, blots were re-probed with Rabbit anti-

GFP primary antibody (Invitrogen) to determine the specificity of the precipitation. Samples

containing RFP alone were heated for 5 minutes at 94°C before SDS-PAGE; samples containing

RFP-DGKη constructs were not heated, because we found that DGKη protein and DGKη

truncation constructs were undetectable on western blots when heated at 94°C.

RESULTS

Mouse DGKη phosphorylates multiple DAG substrates

First, we set out to evaluate whether mouse DGKη isoform 1 was catalytically active

(Fig. 1A shows domain structure of isoform 1, henceforth referred to as DGKη or DGKη1). To

accomplish this, we transfected HEK293 cells with RFP-tagged DGKη or RFP only (control)

expression constructs. One day later, we prepared cell lysates, incubated these lysates with

purified DAG substrates and $[\gamma\text{-}^{32}P]ATP$, then monitored ^{32}P-labeled phosphatadic acid (PA)

formation (Fig. 1B). This *in vitro* assay was previously used to monitor DGK activity (Kanoh et

al., 1992; Ohanian and Heagerty, 1994). We found that kinase reactions containing RFP-DGKη

produced significantly more ^{32}P-PA than reactions containing RFP alone (Fig. 1C) when 500 µM

dioctanoyl (8:0), dilauroyl (12:0), or dioleoyl (18:1) glycerol was used as substrate. Given that

mouse DGKη could phosphorylate multiple DAG substrates, and that 18:1 DAG was previously

used to characterize human DGKη and other DGK isoforms (Murakami et al., 2003), we elected

to use 18:1 DAG for subsequent experiments. Furthermore, we found that 500 µM 18:1 DAG

was a saturating concentration of substrate (Fig. 1D), justifying our use of this DAG

concentration for subsequent *in vitro* kinase reactions.

DGKη increases intracellular calcium responses after GPCR stimulation

Since DGKη is expressed at higher levels in patients with bipolar disorder (Moya et al.,

2010), we next sought to determine if overexpression of DGKη affects endogenous GPCR

signaling. We focused our research on HEK293 cells because they endogenously express the M_3

muscarinic acetylcholine receptor, a $G\alpha_q$-coupled GPCR that mobilizes intracellular calcium

following stimulation with carbachol (Luo et al., 2008). Carbachol causes calcium release by

specifically activating the M_3, but not the M_1, receptor in HEK293 cells (Luo et al., 2008).

Moreover, M_3 receptor desensitization and downstream signaling pathways have been

extensively studied in HEK293 cells (Rumenapp et al., 2001; Luo et al., 2008). After stimulating

with 10 µM carbachol, we found that the calcium mobilization response was enhanced in

HEK293 cells expressing RFP-DGKη compared to RFP alone (Fig. 1E). Based on quantifying

the area under the curve (AUC), the carbachol-evoked calcium response in RFP-DGKη-

expressing cells was 80% greater than in cells expressing RFP alone ($p < 0.001$). However, the

peak amplitude of carbachol-evoked calcium responses in cells expressing RFP alone and RFP-

DGKη was identical (Supplemental Fig. 1), indicating that overexpression of RFP-DGKη

increases the duration, but not the intensity, of carbachol-evoked calcium mobilization. Indeed,

no significant difference in peak amplitudes was observed in the vast majority of calcium

mobilization conditions explored in this work (Supplemental Fig. 1), and the few significant

differences that were observed were very small and without consistent direction. Furthermore,

the N-terminal RFP tag did not affect DGKη activity, as untagged DGKη, HA-DGKη, and

DGKη-mCherry also enhanced carbachol-evoked calcium responses (data not shown; we

identified cells with untagged or HA-tagged DGKη by co-transfecting with Venus, a yellow

fluorescent protein).

We next investigated whether DGKη could increase calcium mobilization downstream of

other $G\alpha_q$-coupled GPCRs. To accomplish this, we stimulated HEK293 cells with 10 µM ATP,

which elicits intracellular calcium mobilization by activating endogenous P2Y receptors (Rittiner

et al., 2012). We found that HEK293 cells expressing RFP-DGKη exhibited elevated ATP-

evoked calcium responses compared to cells expressing RFP alone (Fig. 1F). When quantified

by AUC, ATP-evoked calcium responses in RFP-DGKη-expressing cells were 81% greater than

15

responses in cells expressing RFP alone ($p < 0.01$). These data indicate that overexpression of

DGKη can enhance calcium responses downstream of two different GPCRs. Since calcium

mobilization was more pronounced (longer duration) following endogenous M_3 receptor

activation, we focused the remainder of our experiments on DGKη modulation of M_3 receptor

activation.

DGKη catalytic activity is required to enhance carbachol-evoked calcium mobilization

DGKη, like all Type II DGKs, possesses a split catalytic domain (Sakane et al., 2007).

To determine if DGKη catalytic activity was required to enhance carbachol-evoked calcium

mobilization, we generated two DGKη deletion constructs, DGKη-Δ645 and DGKη-646Δ, each

containing one half of the catalytic domain (Fig. 2A). We also generated DGKη-G389D,

containing a point mutation that is predicted to abolish ATP binding based on homology to other

DGK proteins (Yamada et al., 2003). We found that DGKη-Δ645, DGKη-646Δ, and DGKη-

G389D were expressed (Supplemental Fig. 2) but were catalytically inactive, as they generated

no more ^{32}P-PA than lysates containing RFP alone (Fig. 2B). In contrast, lysates from cells co-

expressing DGKη-Δ645 and DGKη-646Δ displayed specific activity (catalytic activity

normalized for expression – Supplemental Fig. 2) approximately 32% of that of wild-type (WT)

RFP-DGKη (Fig. 2B), suggesting the two halves directly interact. Indeed, we found that RFP-

DGKη-Δ645 co-immunoprecipitated with Venus-DGKη-646Δ (Fig. 2C). This interaction was

specific to DGKη-Δ645 and DGKη-646Δ and did not involve the fluorescent tags or non-specific

binding to the immunoprecipitation beads, as evidenced by controls showing no interaction when

either construct was replaced with a fluorescent protein alone or when the anti-GFP antibody was

replaced with an IgY control (Fig. 2C).

16

Additionally, none of these catalytically dead constructs (DGKη-Δ645, DGKη-646Δ or DGKη-G389D) enhanced calcium mobilization after carbachol stimulation (Fig. 2D). Cells expressing DGKη-646Δ alone appeared unhealthy and displayed a slight reduction in calcium mobilization. In contrast, co-expression of each half of DGKη (RFP-tagged DGKη-Δ645 and Venus-tagged DGKη-646Δ) increased calcium mobilization by 62% (based on AUC measurement, Fig. 2D). These data indicate that DGKη catalytic activity is required to enhance carbachol-evoked calcium mobilization.

We next analyzed calcium mobilization AUC data on a cell-by-cell basis, to determine if the expression level of DGKη correlated with how effectively DGKη enhanced calcium mobilization responses. Notably, there was no relationship between the level of DGKη expression and the extent of calcium mobilization in cells expressing WT DGKη or kinase-dead DGKη-G389D (Fig. 2E). There was also no significant difference in the expression level of WT DGKη and DGKη-G389D across individual cells. Together, these data suggest that the amount of DGKη required to maximally enhance carbachol-evoked calcium mobilization is very small.

We also tested the catalytic activity of several DGKη truncation constructs lacking other structural domains (Fig. 3A), again normalized to their expression in HEK293 cells (Supplemental Fig. 2). We found that the PH domain and C-terminal tail negatively regulated DGKη catalytic activity, as measured using the *in vitro* kinase assay (Fig. 3B). Truncation of either domain increased DGKη specific activity in an additive fashion, and the construct lacking both domains (161Δ961) displayed a specific activity 6-fold higher than WT DGKη (Fig. 3B). The C1 domains were required for catalytic activity in this assay, as both constructs lacking C1 domains were inactive (Fig. 3B). Furthermore, the presence of catalytic activity among the DGKη truncation constructs correlated with the ability to enhance carbachol-evoked calcium

17

mobilization (Fig. 3 B,C). However, this correlation was not quantitative. The DGKη truncation

constructs with greatly increased catalytic activity (compared to WT DGKη) enhanced calcium

mobilization to an equal or only marginally increased extent. These data suggest that beyond a

certain point, increased DGKη catalytic activity does not result in an increased effect upon

calcium mobilization. Lastly, we tested the long splice isoform DGKη2, which contains a C-

terminal sterile alpha motif (SAM) domain (Fig. 3A), in both the *in vitro* kinase and calcium

mobilization assays. We found that DGKη2 had decreased catalytic activity compared to WT

DGKη1 (Fig. 3B) as has been reported previously (Murakami et al., 2003), and produced only a

negligible ($p = 0.057$ compared to RFP alone) enhancement of carbachol-evoked calcium

mobilization (Fig. 3C). As with WT DGKη, we observed no correlation between DGKη

expression and calcium mobilization for any of the DGKη truncation constructs on a cell-by-cell

basis (Supplemental Figure 3).

DGKη does not affect ER calcium loading

 Next, to determine if DGKη enhanced calcium responses by affecting the loading of

intracellular calcium stores, and not GPCR signaling per se, we treated RFP-DGKη-expressing

cells and RFP-expressing controls with 1 µM thapsagargin in the presence of extracellular

calcium. Thapsigargin is a non-competitive SERCA inhibitor that causes the release of

intracellular calcium store contents into the cytosol (Jackson et al., 1988). Calcium release was

not significantly different between cells expressing RFP alone and RFP-DGKη (Fig. 4A),

indicating that DGKη has no effect on the loading of intracellular calcium stores.

 When intracellular calcium stores become depleted, calcium-sensing proteins trigger the

opening of calcium channels in the plasma membrane, allowing the entry of extracellular

calcium, a process known as store-operated calcium entry (Venkatachalam et al., 2002). To

determine if DGKη enhanced calcium mobilization by affecting this process, we stimulated cells

with carbachol in the absence of extracellular calcium (to abolish calcium entry through any

channels or transporters). In the absence of extracellular calcium, carbachol-evoked calcium

mobilization was reduced, particularly in the later stages of the response (compare Fig. 4B to

Fig. 1E). However, overexpression of DGKη still enhanced the calcium response by 77% (based

on AUC measurements) when compared to RFP alone. This effect was nearly identical to the

80% AUC increase in the presence of extracellular calcium (Fig. 1E). Thus, these data indicate

that DGKη enhances the carbachol-evoked calcium response via a mechanism that is not solely

dependent upon the modulation of calcium entry.

DGKη does not translocate after GPCR stimulation

Human DGKη localizes to the cytosol under baseline conditions and translocates to

endosomes after osmotic shock (Murakami et al., 2003; Matsutomo et al., 2013). However,

whether DGKη translocates to the plasma membrane or intracellular compartments following

GPCR stimulation is unknown. Using live cell confocal imaging, we found that mouse DGKη is

localized throughout the cytoplasm in unstimulated cells and did not translocate to the plasma

membrane or to any intracellular compartment after stimulating with 10 µM carbachol at room

temperature (Fig. 5A). This experiment was conducted under conditions that were identical to

those used in the carbachol-evoked calcium mobilization assay, suggesting that the effects of

DGKη on GPCR signaling require little if any translocation of DGKη. Furthermore, we were

unable to detect translocation of DGKη when cells were stimulated with 10 µM or 100 µM

carbachol at 37°C (data not shown). Our inability to detect DGKη translocation was not a

technical limitation, as our mouse DGKη construct rapidly translocated to endosomes after

osmotic shock at room temperature (Fig. 5B), as previously shown using human DGKη

(Murakami et al., 2003; Matsutomo et al., 2013).

DGKη enhances GPCR signaling by attenuating PKC activation

DAG is a canonical activator of conventional and novel isoforms of PKC (Mellor and

Parker, 1998). Additionally, PKC is directly and indirectly involved in the phosphorylation and

subsequent desensitization of GPCRs (Krasel et al., 2001; Kelly et al., 2008; Feng et al., 2011).

Therefore, we hypothesized that DGKη might enhance GPCR signaling by metabolizing DAG

and hence reducing PKC activation. First, we confirmed that acute treatment with 300 nM PMA

could activate PKC in HEK293 cells. PMA is a phorbol ester that is structurally similar to DAG

and potently activates multiple PKC isoforms (Blumberg, 1988), For this control experiment,

we focused on PKCδ because it is highly expressed in HEK293 cells (Leaney et al., 2001) and it

is a Ca^{2+}-insensitive isoform of PKC (Mellor and Parker, 1998). We found that PMA induced a

rapid (within 2 minutes) translocation of PKCδ to the plasma membrane (Fig. 6A). However,

300 nM PMA did not induce translocation of overexpressed RFP-DGKη to the plasma

membrane or any other cellular compartment during the same time frame (data not shown). We

then measured calcium mobilization after stimulating RFP- and RFP-DGKη-expressing cells

with 300 μM PMA followed immediately by 10 μM carbachol. Stimulation with 300 nM PMA

profoundly accelerated the return of carbachol-evoked calcium mobilization to baseline (Fig. 6B,

compare to Fig. 1E). Furthermore, the carbachol-evoked calcium responses were identical in

cells expressing RFP alone and RFP-DGKη when PKC was acutely activated with 300 nM PMA

(Fig. 6B). In contrast, stimulation of RFP-expressing cells with 300 nM PMA alone did not

evoke a calcium response (Fig. 6B). Taken together, these data indicate that PKC activation

blunts GPCR signaling in HEK293 cells and occludes the effect of DGKη.

We next determined whether pharmacological inhibition of PKC activity would enhance

GPCR signaling, using the cell-permeable PKC inhibitor bisindolylmaleimide I (BIM I) (Toullec

et al., 1991). We found that carbachol-evoked calcium mobilization in RFP-expressing HEK293

cells was dramatically enhanced after preincubation with 1 µM BIM I (Fig. 6C). This effect was

nearly identical to that observed after expression of RFP-DGKη (compare Fig. 6C with Fig. 1E).

Indeed, BIM I pretreatment yielded an 81% increase in calcium responses (based on AUC

measurements), essentially the same as the 80% AUC increase observed after RFP-DGKη

expression (Fig. 1E). Furthermore, carbachol-evoked calcium responses were indistinguishable

in RFP- and RFP-DGKη-expressing cells after pretreatment with BIM I (Fig. 6C). A different

PKC inhibitor (1 µM Gö6976) also enhanced calcium mobilization to nearly the same extent in

RFP-expressing and RFP-DGKη-expressing cells (Fig. 6D), although the kinetics were different

when compared to BIM I, possibly because Gö6976 is selective for the Ca^{2+}-sensitive PKCα and

PKCβ isoforms (Martiny-Baron et al., 1993). Taken together, these data show that

pharmacological inhibition of PKC activity both mimics the effect of DGKη and prevents

overexpressed DGKη from enhancing calcium mobilization further. The latter finding suggests

that PKC inhibitors and overexpressed DGKη work via a similar mechanism—by inhibiting

PKC directly (inhibitors) or indirectly (by depleting the PKC activator DAG). Thus, these data

suggest that DGKη potentiates GPCR signaling via PKC, likely by reducing the levels of a PKC

activator (DAG) and attenuating PKC activity.

DISCUSSION

Collectively, our data suggest a model for how DGKη enhances GPCR signaling (Fig. 7). Stimulation of $G\alpha_q$-coupled GPCRs leads to the activation of phospholipase C (PLC) and the hydrolysis of phosphatidylinositol 4,5-bisphosphate (PIP_2) into inositol 1,4,5-trisphosphate (IP_3) and DAG. IP_3 subsequently induces the release of calcium from endoplasmic reticulum calcium stores, raising the cytosolic concentration of Ca^{2+}. In cells not overexpressing DGKη (Fig. 7A), DAG activates PKC, leading to the phosphorylation and desensitization of the activated GPCR, followed by termination of GPCR signaling (Tang et al., 1995; Gereau and Heinemann, 1998; Kelly et al., 2008). However, in cells overexpressing DGKη, DAG is phosphorylated to PA, leading to a decreased level of PKC activation (Fig. 7B, red). This causes a decrease in the rate of GPCR phosphorylation and desensitization, resulting in enhanced GPCR signaling (as evidenced by elevated intracellular calcium release).

During activation, PKC isoforms translocate to the plasma membrane (Nishizuka, 1984), and are autophosphorylated at multiple amino acid residues (Keranen et al., 1995; Newton, 2003). We attempted to measure PKC activation directly via: 1) PKCδ immunostaining (Fig. 6A), 2) membrane/cytosol fractionation and PKCδ western blotting (Brown et al., 2005), 3) anti-phospho-PKCδ western blotting (Sumandea et al., 2008), 4) anti-pan-phospho-PKC western blotting (Iwabu et al., 2004), 5) a GFP biosensor based on the C1 domains of PKCγ (Oancea et al., 1998), and 6) a FRET biosensor of PKC activity (Violin et al., 2003). Unfortunately, we did not observe endogenous PKC activation with any of these techniques after stimulating endogenous M_3 receptors with carbachol, and were therefore unable to directly measure the effect of DGKη on endogenous PKC activity. This did not reflect technical limitations, as we did observe endogenous PKCδ activation after direct stimulation with PMA (Fig. 6A). Instead,

22

our inability to directly measure endogenous PKC activity suggests very little PKC is activated

when endogenous receptors are stimulated, likely due to a low level of DAG release. Indeed, we

observed that only a minimal level of DGKη expression results in the full enhancing effect on

calcium mobilization (Fig. 2E), and that increased DGKη catalytic activity does not increase this

effect beyond a certain point (Fig. 3C). Both these observations are entirely consistent with

DGKη activity being constrained by a low level of available DAG substrate. In further support

of this possibility, we did not detect an increase in DAG levels after activating the endogenous

M_3 receptor with carbachol (using a sensitive DAG biosensor, Upward DAG2; data not shown)

(Tewson et al., 2013).

Previous studies that measured PKC activity employed overexpressed receptors (Iwabu et

al., 2004; Brown et al., 2005). It is well-documented that overexpressed receptors activate

signaling pathways at non-physiological (excessive) levels relative to endogenous receptor

activation (Dickson et al., 2013). This is precisely why we used endogenous M_3 receptors and a

sub-EC_{50} concentration of carbachol (Luo et al., 2008) in our signaling experiments, to probe

potential negative and positive modulation at physiological levels of GPCR activation. Although

we were unable to directly measure changes in endogenous PKC activity when stimulating with

carbachol, modulation of PKC activity clearly mediates the effect of DGKη on GPCR signaling,

as both activation (Fig. 6B) and inhibition (Fig. 6C) of PKC blocked overexpressed DGKη from

enhancing endogenous M_3 receptor activation.

It is well-established that PKC activation leads to desensitization of GPCRs (Tang et al.,

1995; Gereau and Heinemann, 1998; Kelly et al., 2008). Based on this literature, we suggest that

overexpression of DGKη enhances GPCR signaling by attenuating PKC-mediated

phosphorylation and desensitization of GPCRs (Fig. 7). Such a mechanism should have a greater

effect on the duration of calcium responses than the intensity, consistent with our findings (Fig. 1 E,F, Supplemental Fig. 1). Likewise, cholinergic stimulation of cells expressing a phosphorylation-deficient M_3 receptor resulted in enhanced calcium mobilization when compared to cells expressing wild-type M_3 receptor (Kong et al., 2010), resembling the effect of overexpressed DGKη following M_3 receptor activation. However, it remains possible that another mechanism downstream of PKC, such as modulation of calcium transporter activity (Usachev et al., 2002; Usachev et al., 2006), is responsible for the increased duration of calcium responses observed in DGKη-expressing cells.

Note that M_3 receptor internalization (as distinct from desensitization) is not likely to be involved in DGKη-mediated modulation of receptor signaling, as internalization of the M_3 receptor is very slow (hours), even during continuous stimulation with an extremely high concentration of carbachol (Thangaraju and Sawyer, 2011). Although PKC directly phosphorylates some GPCRs (Kelly et al., 2008; Feng et al., 2011), phosphorylation of the M_3 receptor in HEK293 cells could be indirect, through the activation of G protein-coupled receptor kinases (GRKs). In HEK293 cells, M_3 receptor activity is regulated by GRKs 2, 3, and 6 (Luo et al., 2008), at least one of which is activated by PKC (Krasel et al., 2001). Interestingly, GRK3 is also genetically linked to BPD (Rao et al., 2009), suggesting that dysregulation of GPCR signaling is important in the pathology of BPD.

Other DGK isoforms regulate PKC and receptor signaling. For example, disruption of the gene encoding DGKδ leads to DAG accumulation and enhanced PKC activity and EGFR phosphorylation (Crotty et al., 2006), culminating in a PKC-dependent increase in EGFR ubiquitination and degradation (Cai et al., 2010). DGKs also regulate inter-receptor desensitization pathways, as DGKθ attenuates bradykinin-evoked, PKC-mediated

phosphorylation of EGFR, a phosphorylation event that is linked to EGFR desensitization (van Baal et al., 2012). Interestingly, EGFR is a receptor tyrosine kinase, indicating that regulation of receptor signaling by DGKs is not limited to GPCRs. These studies, when combined with our current study, suggest that multiple members of the DGK enzyme family can regulate PKC activity and receptor signaling.

Lastly, our study provides new insights into how alterations in DGKη might affect cellular signaling in patients with BPD. Numerous genome-wide association studies have linked single nucleotide polymorphisms (SNPs) within *DGKH* to BPD (Baum et al., 2008; Squassina et al., 2009; Takata et al., 2011; Weber et al., 2011; Yosifova et al., 2011; Zeng et al., 2011); although whether these SNPs increase, decrease or have no effect on *DGKH* expression is unknown. In one study, *DGKH* was found to be expressed at higher levels in post-mortem tissues from patients with BPD than unaffected controls (Moya et al., 2010), suggesting that DGKη enzymatic activity might also be elevated. Given that overexpression of DGKη enhanced GPCR signaling in a model cell line, it is tempting to speculate that GPCR signaling might be dysregulated in other cell types when DGKη activity is increased or decreased. Ultimately, future studies will be needed to delineate precisely how DGKη activity is altered in BPD patients and how such alterations affect PKC and GPCR signaling in neurons and in animal models of BPD.

ACKNOWLEDGMENTS

AUTHOR CONTRIBUTIONS

Participated in research design: Rittiner and Zylka

Conducted experiments: Rittiner and Brings

Performed data analysis: Rittiner

Wrote or contributed to the writing of the manuscript: Rittiner, Brings, and Zylka

REFERENCES

Avissar S, Schreiber G, Danon A and Belmaker RH (1988) Lithium inhibits adrenergic and cholinergic increases in GTP binding in rat cortex. *Nature* **331**(6155):440-442.

Baum AE, Akula N, Cabanero M, Cardona I, Corona W, Klemens B, Schulze TG, Cichon S, Rietschel M, Nothen MM, Georgi A, Schumacher J, Schwarz M, Abou Jamra R, Hofels S, Propping P, Satagopan J, Detera-Wadleigh SD, Hardy J and McMahon FJ (2008) A genome-wide association study implicates diacylglycerol kinase eta (DGKH) and several other genes in the etiology of bipolar disorder. *Mol Psychiatry* **13**(2):197-207.

Blumberg PM (1988) Protein kinase C as the receptor for the phorbol ester tumor promoters: sixth Rhoads memorial award lecture. *Cancer Res* **48**(1):1-8.

Brown SG, Thomas A, Dekker LV, Tinker A and Leaney JL (2005) PKC-delta sensitizes Kir3.1/3.2 channels to changes in membrane phospholipid levels after M3 receptor activation in HEK-293 cells. *Am J Physiol Cell Physiol* **289**(3):C543-556.

Cai J, Crotty TM, Reichert E, Carraway KL, 3rd, Stafforini DM and Topham MK (2010) Diacylglycerol kinase delta and protein kinase C(alpha) modulate epidermal growth factor receptor abundance and degradation through ubiquitin-specific protease 8. *J Biol Chem* **285**(10):6952-6959.

Catapano LA and Manji HK (2007) G protein-coupled receptors in major psychiatric disorders. *Biochim Biophys Acta* **1768**(4):976-993.

Crotty T, Cai J, Sakane F, Taketomi A, Prescott SM and Topham MK (2006) Diacylglycerol kinase delta regulates protein kinase C and epidermal growth factor receptor signaling. *Proc Natl Acad Sci U S A* **103**(42):15485-15490.

Dickson EJ, Falkenburger BH and Hille B (2013) Quantitative properties and receptor reserve of the IP(3) and calcium branch of G(q)-coupled receptor signaling. *J Gen Physiol* **141**(5):521-535.

Feng B, Li Z and Wang JB (2011) Protein kinase C-mediated phosphorylation of the mu-opioid receptor and its effects on receptor signaling. *Mol Pharmacol* **79**(4):768-775.

Friedman E and Wang HY (1996) Receptor-mediated activation of G proteins is increased in postmortem brains of bipolar affective disorder subjects. *J Neurochem* **67**(3):1145-1152.

Gereau RWt and Heinemann SF (1998) Role of protein kinase C phosphorylation in rapid desensitization of metabotropic glutamate receptor 5. *Neuron* **20**(1):143-151.

Gregg LC, Jung KM, Spradley JM, Nyilas R, Suplita RL, 2nd, Zimmer A, Watanabe M, Mackie K, Katona I, Piomelli D and Hohmann AG (2012) Activation of type 5 metabotropic glutamate receptors and diacylglycerol lipase-alpha initiates 2-arachidonoylglycerol formation and endocannabinoid-mediated analgesia. *J Neurosci* **32**(28):9457-9468.

Hahn CG, Umapathy, Wang HY, Koneru R, Levinson DF and Friedman E (2005) Lithium and valproic acid treatments reduce PKC activation and receptor-G protein coupling in platelets of bipolar manic patients. *J Psychiatr Res* **39**(4):355-363.

Iwabu A, Smith K, Allen FD, Lauffenburger DA and Wells A (2004) Epidermal growth factor induces fibroblast contractility and motility via a protein kinase C delta-dependent pathway. *J Biol Chem* **279**(15):14551-14560.

Jackson TR, Patterson SI, Thastrup O and Hanley MR (1988) A novel tumour promoter, thapsigargin, transiently increases cytoplasmic free Ca2+ without generation of inositol phosphates in NG115-401L neuronal cells. *Biochem J* **253**(1):81-86.

28

Jenkins GH, Fisette PL and Anderson RA (1994) Type I phosphatidylinositol 4-phosphate 5-
kinase isoforms are specifically stimulated by phosphatidic acid. *J Biol Chem*
269(15):11547-11554.

Kanoh H, Sakane F and Yamada K (1992) Diacylglycerol kinase isozymes from brain and
lymphoid tissues. *Methods Enzymol* **209**:162-172.

Kelly E, Bailey CP and Henderson G (2008) Agonist-selective mechanisms of GPCR
desensitization. *Br J Pharmacol* **153 Suppl 1**:S379-388.

Keranen LM, Dutil EM and Newton AC (1995) Protein kinase C is regulated in vivo by three
functionally distinct phosphorylations. *Curr Biol* **5**(12):1394-1403.

Klauck TM, Xu X, Mousseau B and Jaken S (1996) Cloning and characterization of a
glucocorticoid-induced diacylglycerol kinase. *J Biol Chem* **271**(33):19781-19788.

Kong KC, Butcher AJ, McWilliams P, Jones D, Wess J, Hamdan FF, Werry T, Rosethorne EM,
Charlton SJ, Munson SE, Cragg HA, Smart AD and Tobin AB (2010) M3-muscarinic
receptor promotes insulin release via receptor phosphorylation/arrestin-dependent
activation of protein kinase D1. *Proc Natl Acad Sci U S A* **107**(49):21181-21186.

Krasel C, Dammeier S, Winstel R, Brockmann J, Mischak H and Lohse MJ (2001)
Phosphorylation of GRK2 by protein kinase C abolishes its inhibition by calmodulin. *J
Biol Chem* **276**(3):1911-1915.

Leaney JL, Dekker LV and Tinker A (2001) Regulation of a G protein-gated inwardly rectifying
K+ channel by a Ca(2+)-independent protein kinase C. *J Physiol* **534**(Pt. 2):367-379.

Lucas P, Ukhanov K, Leinders-Zufall T and Zufall F (2003) A diacylglycerol-gated cation
channel in vomeronasal neuron dendrites is impaired in TRPC2 mutant mice: mechanism
of pheromone transduction. *Neuron* **40**(3):551-561.

Luo J, Busillo JM and Benovic JL (2008) M3 muscarinic acetylcholine receptor-mediated signaling is regulated by distinct mechanisms. *Mol Pharmacol* **74**(2):338-347.

Martiny-Baron G, Kazanietz MG, Mischak H, Blumberg PM, Kochs G, Hug H, Marme D and Schachtele C (1993) Selective inhibition of protein kinase C isozymes by the indolocarbazole Go 6976. *J Biol Chem* **268**(13):9194-9197.

Matsutomo D, Isozaki T, Sakai H and Sakane F (2013) Osmotic shock-dependent redistribution of diacylglycerol kinase eta1 to non-ionic detergent-resistant membrane via pleckstrin homology and C1 domains. *J Biochem* **153**(2):179-190.

Mellor H and Parker PJ (1998) The extended protein kinase C superfamily. *Biochem J* **332 (Pt 2)**:281-292.

Merida I, Avila-Flores A and Merino E (2008) Diacylglycerol kinases: at the hub of cell signalling. *Biochem J* **409**(1):1-18.

Moya PR, Murphy DL, McMahon FJ and Wendland JR (2010) Increased gene expression of diacylglycerol kinase eta in bipolar disorder. *Int J Neuropsychopharmacol* **13**(8):1127-1128.

Murakami T, Sakane F, Imai S, Houkin K and Kanoh H (2003) Identification and characterization of two splice variants of human diacylglycerol kinase eta. *J Biol Chem* **278**(36):34364-34372.

Nakano T, Iravani A, Kim M, Hozumi Y, Lohse M, Reichert E, Crotty TM, Stafforini DM and Topham MK (2013) Diacylglycerol kinase eta modulates oncogenic properties of lung cancer cells. *Clin Transl Oncol*. **16**(1):29-35.

Newton AC (2003) Regulation of the ABC kinases by phosphorylation: protein kinase C as a paradigm. *Biochem J* **370**(Pt 2):361-371.

Nishizuka Y (1984) The role of protein kinase C in cell surface signal transduction and tumour promotion. *Nature* **308**(5961):693-698.

Oancea E, Teruel MN, Quest AF and Meyer T (1998) Green fluorescent protein (GFP)-tagged cysteine-rich domains from protein kinase C as fluorescent indicators for diacylglycerol signaling in living cells. *J Cell Biol* **140**(3):485-498.

Ohanian J and Heagerty AM (1994) Membrane-associated diacylglycerol kinase activity is increased by noradrenaline, but not by angiotensin II, in arterial smooth muscle. *Biochem J* **300 (Pt 1)**:51-56.

Pantazopoulos H, Stone D, Walsh J and Benes FM (2004) Differences in the cellular distribution of D1 receptor mRNA in the hippocampus of bipolars and schizophrenics. *Synapse* **54**(3):147-155.

Rao JS, Rapoport SI and Kim HW (2009) Decreased GRK3 but not GRK2 expression in frontal cortex from bipolar disorder patients. *Int J Neuropsychopharmacol* **12**(6):851-860.

Rittiner JE, Korboukh I, Hull-Ryde EA, Jin J, Janzen WP, Frye SV and Zylka MJ (2012) AMP is an adenosine A1 receptor agonist. *J Biol Chem* **287**(8):5301-5309.

Rumenapp U, Asmus M, Schablowski H, Woznicki M, Han L, Jakobs KH, Fahimi-Vahid M, Michalek C, Wieland T and Schmidt M (2001) The M3 muscarinic acetylcholine receptor expressed in HEK-293 cells signals to phospholipase D via G12 but not Gq-type G proteins: regulators of G proteins as tools to dissect pertussis toxin-resistant G proteins in receptor-effector coupling. *J Biol Chem* **276**(4):2474-2479.

Sakane F, Imai S, Kai M, Yasuda S and Kanoh H (2007) Diacylglycerol kinases: why so many of them? *Biochim Biophys Acta* **1771**(7):793-806.

Squassina A, Manchia M, Congiu D, Severino G, Chillotti C, Ardau R, Piccardi M and Zompo MD (2009) The diacylglycerol kinase eta gene and bipolar disorder: a replication study in a Sardinian sample. *Mol Psychiatry* **14**(4):350-351.

Sumandea MP, Rybin VO, Hinken AC, Wang C, Kobayashi T, Harleton E, Sievert G, Balke CW, Feinmark SJ, Solaro RJ and Steinberg SF (2008) Tyrosine phosphorylation modifies protein kinase C delta-dependent phosphorylation of cardiac troponin I. *J Biol Chem* **283**(33):22680-22689.

Takata A, Kawasaki H, Iwayama Y, Yamada K, Gotoh L, Mitsuyasu H, Miura T, Kato T, Yoshikawa T and Kanba S (2011) Nominal association between a polymorphism in DGKH and bipolar disorder detected in a meta-analysis of East Asian case-control samples. *Psychiatry Clin Neurosci* **65**(3):280-285.

Tang H, Shirai H and Inagami T (1995) Inhibition of protein kinase C prevents rapid desensitization of type 1B angiotensin II receptor. *Circ Res* **77**(2):239-248.

Tewson PH, Quinn AM and Hughes TE (2013) A Multiplexed Fluorescent Assay for Independent Second-Messenger Systems: Decoding GPCR Activation in Living Cells. *J Biomol Screen* **18**(7):797-806.

Thangaraju A and Sawyer GW (2011) Comparison of the kinetics and extent of muscarinic M1-M5 receptor internalization, recycling and downregulation in Chinese hamster ovary cells. *Eur J Pharmacol* **650**(2-3):534-543.

Toullec D, Pianetti P, Coste H, Bellevergue P, Grand-Perret T, Ajakane M, Baudet V, Boissin P, Boursier E, Loriolle F and et al. (1991) The bisindolylmaleimide GF 109203X is a potent and selective inhibitor of protein kinase C. *J Biol Chem* **266**(24):15771-15781.

Usachev YM, DeMarco SJ, Campbell C, Strehler EE and Thayer SA (2002) Bradykinin and ATP accelerate Ca(2+) efflux from rat sensory neurons via protein kinase C and the plasma membrane Ca(2+) pump isoform 4. *Neuron* **33**(1):113-122.

Usachev YM, Marsh AJ, Johanns TM, Lemke MM and Thayer SA (2006) Activation of protein kinase C in sensory neurons accelerates Ca2+ uptake into the endoplasmic reticulum. *J Neurosci* **26**(1):311-318.

van Baal J, de Widt J, Divecha N and van Blitterswijk WJ (2012) Diacylglycerol kinase theta counteracts protein kinase C-mediated inactivation of the EGF receptor. *Int J Biochem Cell Biol* **44**(11):1791-1799.

van Blitterswijk WJ and Houssa B (2000) Properties and functions of diacylglycerol kinases. *Cell Signal* **12**(9-10):595-605.

Venkatachalam K, van Rossum DB, Patterson RL, Ma HT and Gill DL (2002) The cellular and molecular basis of store-operated calcium entry. *Nat Cell Biol* **4**(11):E263-272.

Violin JD, Zhang J, Tsien RY and Newton AC (2003) A genetically encoded fluorescent reporter reveals oscillatory phosphorylation by protein kinase C. *J Cell Biol* **161**(5):899-909.

Weber H, Kittel-Schneider S, Gessner A, Domschke K, Neuner M, Jacob CP, Buttenschon HN, Boreatti-Hummer A, Volkert J, Herterich S, Baune BT, Gross-Lesch S, Kopf J, Kreiker S, Nguyen TT, Weissflog L, Arolt V, Mors O, Deckert J, Lesch KP and Reif A (2011) Cross-disorder analysis of bipolar risk genes: further evidence of DGKH as a risk gene for bipolar disorder, but also unipolar depression and adult ADHD. *Neuropsychopharmacology* **36**(10):2076-2085.

Yamada K, Sakane F, Imai S, Tsushima S, Murakami T and Kanoh H (2003) Regulatory role of diacylglycerol kinase gamma in macrophage differentiation of leukemia cells. *Biochem Biophys Res Commun* **305**(1):101-107.

Yosifova A, Mushiroda T, Kubo M, Takahashi A, Kamatani Y, Kamatani N, Stoianov D, Vazharova R, Karachanak S, Zaharieva I, Dimova I, Hadjidekova S, Milanova V, Madjirova N, Gerdjikov I, Tolev T, Poryazova N, O'Donovan MC, Owen MJ, Kirov G, Toncheva D and Nakamura Y (2011) Genome-wide association study on bipolar disorder in the Bulgarian population. *Genes Brain Behav* **10**(7):789-797.

Young LT, Li PP, Kish SJ, Siu KP, Kamble A, Hornykiewicz O and Warsh JJ (1993) Cerebral cortex Gs alpha protein levels and forskolin-stimulated cyclic AMP formation are increased in bipolar affective disorder. *J Neurochem* **61**(3):890-898.

Zeng Z, Wang T, Li T, Li Y, Chen P, Zhao Q, Liu J, Li J, Feng G, He L and Shi Y (2011) Common SNPs and haplotypes in DGKH are associated with bipolar disorder and schizophrenia in the Chinese Han population. *Mol Psychiatry* **16**(5):473-475.

FOOTNOTES

FIGURE LEGENDS

Figure 1. Mouse DGKη is catalytically active and enhances GPCR signaling. A) Domain architecture of DGKη. PH = Pleckstrin Homology. C1 = PKC homology domain 1. Scale bar; aa = amino acid. B) Schematic of the reaction forming ^{32}P-labeled PA from DAG and radiolabeled ATP. C) Lysates from HEK293 cells expressing (black) RFP alone or (red) RFP-DGKη were incubated with the indicated DAG substrates, each at 500 µM. D) ^{32}P-PA production from reactions containing the indicated concentrations of 18:1 DAG, catalyzed by lysates from HEK293 cells expressing RFP-DGKη. E and F) Calcium mobilization in HEK293 cells expressing (black) RFP alone or (red) RFP-DGKη after stimulation with (E) 10 µM carbachol or (F) 10 µM ATP. AUC measurements extended for 4 minutes from agonist addition. Data in (C) and (D) are the average of two experiments performed in duplicate. Data in E and F are the average of three independent experiments; n = 41-104 cells per condition. **, $p < 0.01$; ***, $p < 0.001$ when compared with RFP alone (unpaired t test). All data, including calcium traces, are presented as means ± S.E.

Figure 2. DGKη catalytic activity is required to enhance GPCR signaling. A) Structure of the DGKη constructs used. DGKη-G389D contains a point mutation in catalytic domain A. All DGKη constructs were N-terminally tagged with RFP unless otherwise noted. B) Production of ^{32}P-PA in reactions containing the indicated DGKη constructs, using 500 µM 18:1 DAG as substrate. Data were normalized to DGKη expression, which was assessed by western blotting against RFP, then normalized so that RFP alone = 0 and WT DGKη = 1. Data are the average of two experiments performed in duplicate. C) Lysates from HEK293 cells expressing RFP-tagged DGKη-Δ645 and Venus-tagged DGKη-646Δ or fluorescent protein controls were

immunoprecipitated using an anti-GFP antibody or an IgY control. Input and precipitated

fractions were then run on SDS-PAGE and blotted using an anti-RFP antibody. The blot was

later re-probed with an anti-GFP antibody to verify the specificity of the immunoprecipitation.

D) AUC measurements of calcium mobilization in HEK293 cells expressing the indicated

DGKη constructs after stimulation with 10 µM carbachol, normalized such that RFP alone = 1.

AUC data for the RFP and WT DGKη conditions are also presented, in non-normalized form, in

Fig. 1E. Data are the average of three to six independent experiments. n = 58-162 cells per

condition, except DGKη-646Δ, where n = 23. E) Scatter plot comparing calcium mobilization

AUC measurements to DGKη expression levels in individual HEK293 cells expressing (red) WT

DGKη or (gray) DGKη-G389D. Horizontal dashed line indicates average level of calcium

mobilization in HEK293 cells expressing RFP alone. *, $p < 0.05$; ***, $p < 0.001$ when compared

with RFP alone. #, $p < 0.05$; ##, $p < 0.01$ when compared with WT DGKη. Unpaired t tests

were used to compare data. All data are presented as means ± S.E.

Figure 3. Catalytic activity and signaling effects of additional DGKη truncation constructs.

A) Domain architecture of the indicated DGKη constructs. All constructs were N-terminally

tagged with RFP. B) Production of ^{32}P-PA in reactions with the indicated DGKη constructs,

using 500 µM 18:1 DAG as substrate. Data were normalized to DGKη expression, which was

assessed by western blotting against RFP, then normalized so that RFP alone = 0 and WT DGKη

= 1. Data are the average of two experiments performed in duplicate. C) AUC measurements of

calcium mobilization in HEK293 cells expressing the indicated DGKη constructs after

stimulation with 10 µM carbachol, normalized such that RFP alone = 1. Data are the average of

three to six independent experiments. n = 75-209 cells per condition. *, $p < 0.05$; **, $p < 0.01$;

***, $p < 0.001$ when compared with RFP alone. #, $p < 0.05$; ##, $p < 0.01$; ###, $p < 0.001$ when

compared with WT DGKη. Unpaired t tests were used to compare data. All data are presented

as means ± S.E.

Figure 4. DGKη does not affect intracellular calcium stores. Calcium mobilization in

HEK293 cells expressing (black) RFP alone or (red) RFP-DGKη after (A) stimulation with 1 µM

thapsigargin or (B) stimulation with 10 µM carbachol in the absence of extracellular calcium.

AUC measurements extended 8 minutes (A) or 4 minutes (B) after stimulation. Data are the

average of two (A) or five (B) independent experiments. n = 69-190 cells per condition. ***, p

< 0.001 when compared with RFP alone (unpaired t test). All data, including calcium traces, are

presented as means ± S.E.

Figure 5. DGKη does not translocate within cells after GPCR stimulation. Confocal images

of live HEK293 cells expressing RFP-DGKη after stimulation with (A) 10 µM carbachol or (B)

500 mM sorbitol for the indicated times. Cell culture and imaging conditions were identical to

those used in calcium mobilization experiments. Panel A shows cells from independent

experiments.

Figure 6. DGKη enhances GPCR signaling via PKC. A) PKCδ translocation following

PMA stimulation. Confocal images of HEK293 cells after treatment with (left) vehicle or (right)

300 nM PMA for 2 minutes. Cells were fixed, immunostained with an anti-PKCδ antibody

(green), and counterstained with DRAQ5 nuclear dye (blue). B) Calcium mobilization in

HEK293 cells expressing (black, blue) RFP alone or (red) RFP-DGKη after stimulation with

38

(black, red) 300 nM PMA followed by 10 µM carbachol, or (blue) 300 nM PMA alone. AUC measurements extended 80 seconds from final agonist addition. Data are the average of two (PMA alone) or three (PMA + carbachol) independent experiments. n = 49-83 cells per condition. C and D) Calcium mobilization in HEK293 cells expressing (black, blue) RFP alone or (red) RFP-DGKη after pretreatment with (blue, red) 1 µM PKC inhibitor (C) BIM I or (D) Gö6976. Cells were stimulated with 10 µM carbachol, and AUC measurements extended 4 minutes from agonist addition. Data in (C) are the average of five independent experiments; n = 140-198 cells per condition. Data in (D) are the average of three independent experiments; n = 85-148 cells per condition. ***, $p < 0.001$ when compared with RFP in the absence of PKC inhibitor. ##, $p < 0.01$ when compared with RFP plus Gö6976. Unpaired t tests were used to compare data. All data, including calcium traces, are presented as means ± S.E.

Figure 7. Model showing how DGKη enhances Gα$_q$-coupled GPCR signaling. A) Activation of Gα$_q$-coupled GPCRs leads to the stimulation of PLC-catalyzed hydrolysis of PIP$_2$ and the release of IP$_3$ and DAG. IP$_3$ activates IP$_3$ receptors on the endoplasmic reticulum, resulting in the release of calcium from intracellular calcium stores. Concurrently, DAG activates conventional and novel isoforms of PKC, leading to the phosphorylation of activated GPCRs, resulting in receptor desensitization and the attenuation of GPCR signaling. B) After receptor activation, overexpressed DGKη reduces the pool of free DAG by converting it into PA, thus suppressing the activation of PKC. As described in the literature (see Discussion), reduced PKC activity attenuates GPCR desensitization. This leads to enhanced IP$_3$ and intracellular calcium release following receptor activation.

Figure 1

# Figure 2

Figure 3

Figure 4

A

1 µM Thapsigargin

Intracellular Ca^{2+} Δ(F340/F380)

Time (s)

RFP Only
RFP-DGKη

Area Under Curve (F340/F380) x s

RFP Only   RFP-DGKη

B

10 µM Carbachol

Intracellular Ca^{2+} Δ(F340/F380)

$0\ [Ca^{2+}]_e$

Time (s)

RFP Only
RFP-DGKη

Area Under Curve (F340/F380) x s

***

RFP Only   RFP-DGKη

Figure 5

A
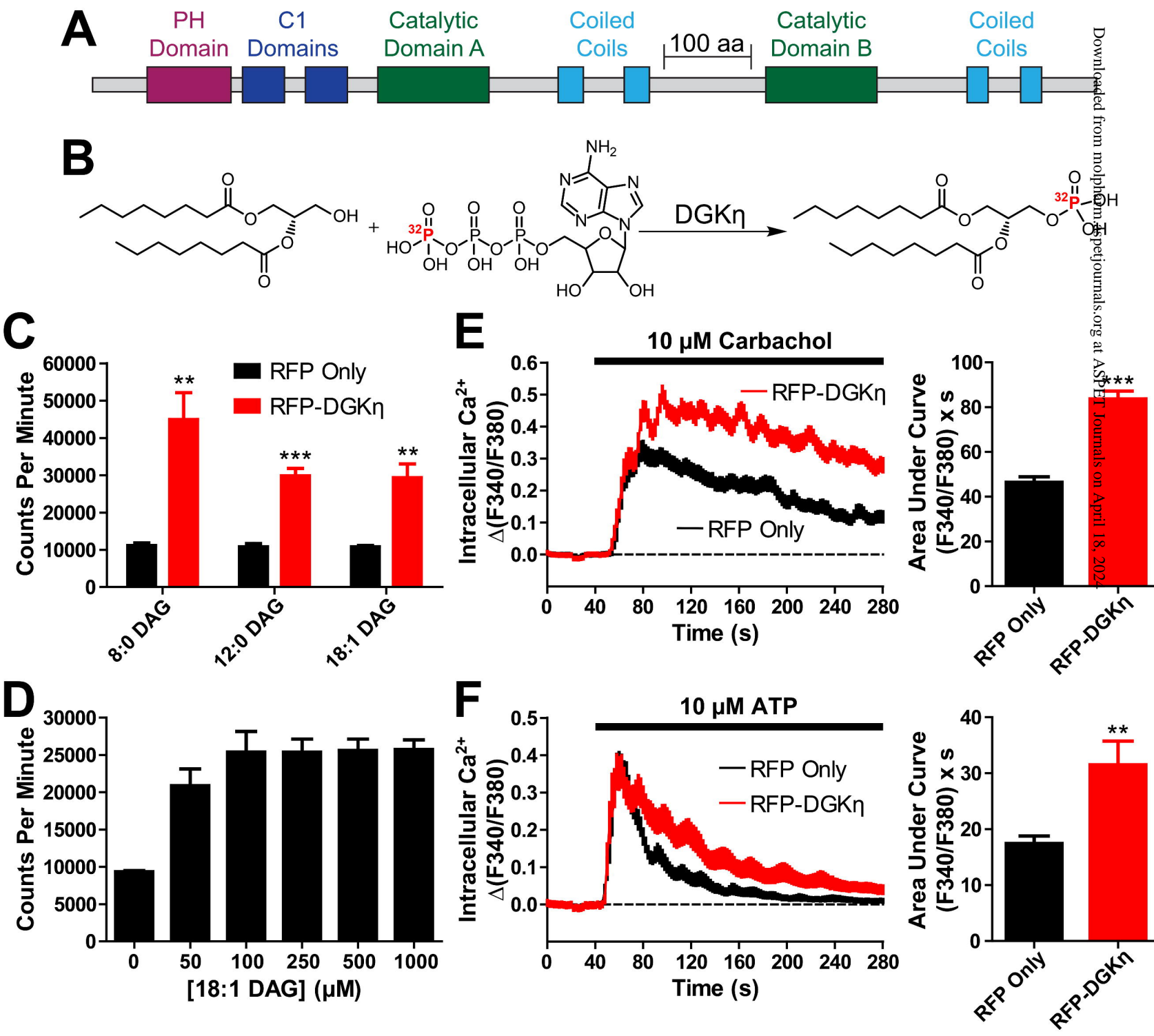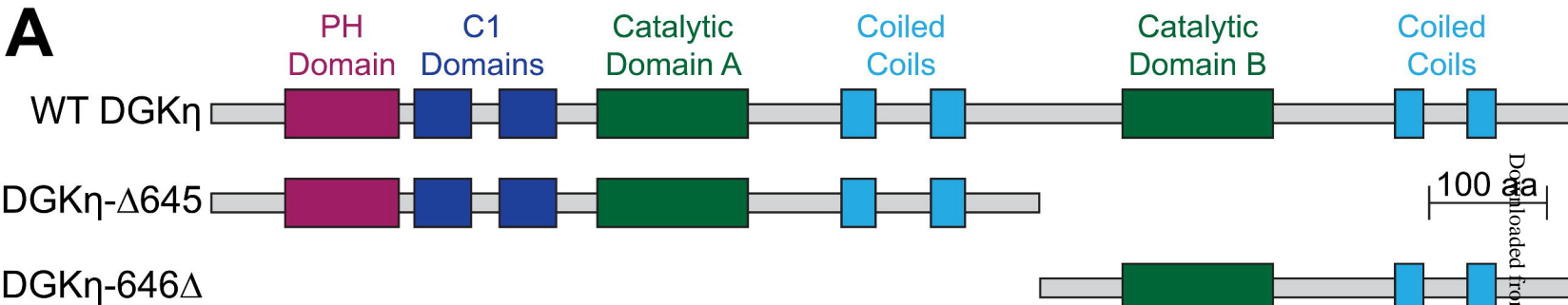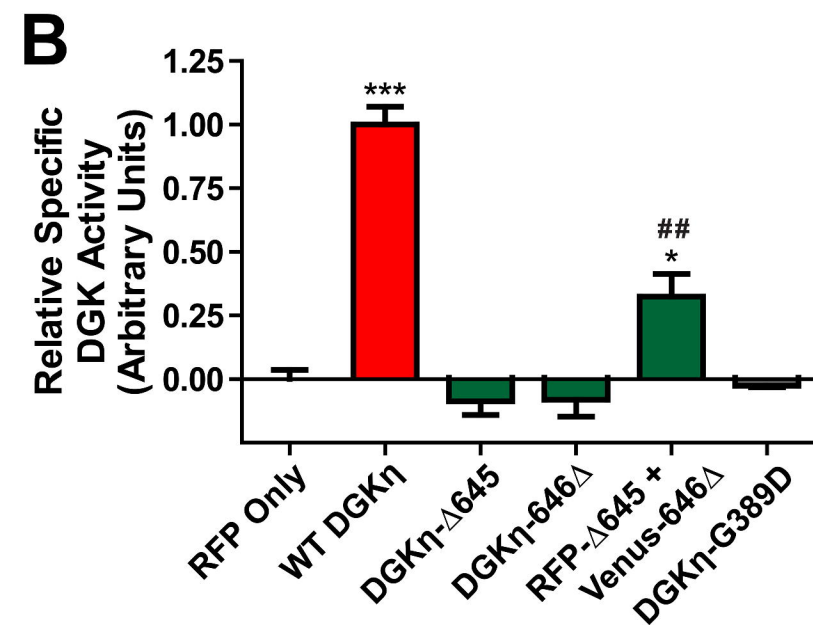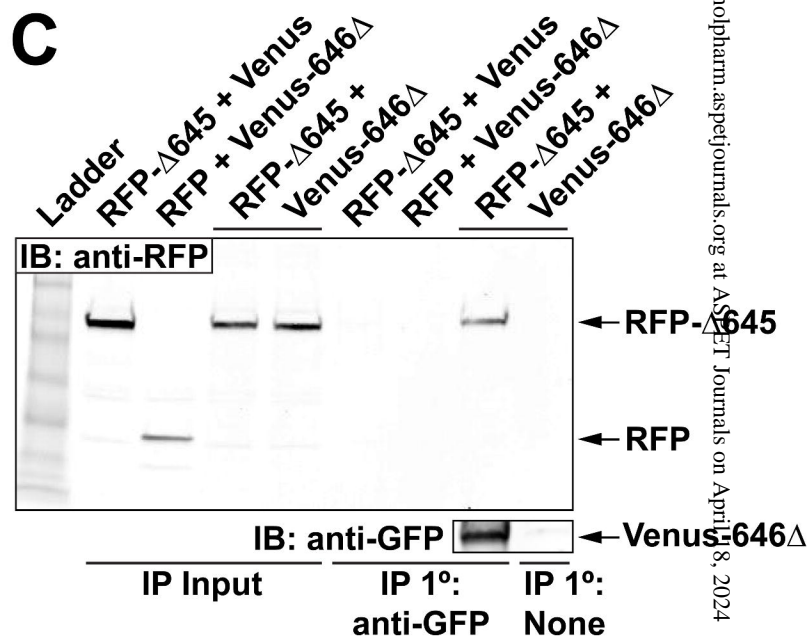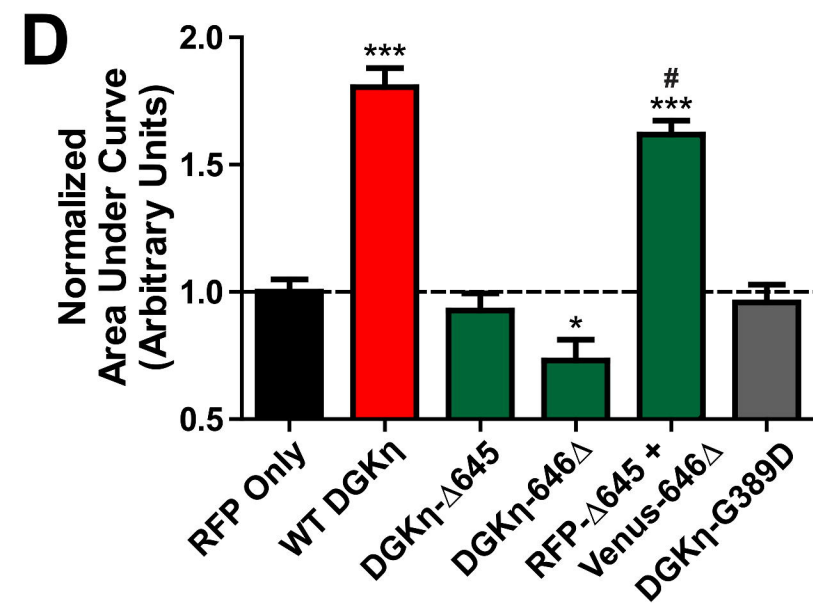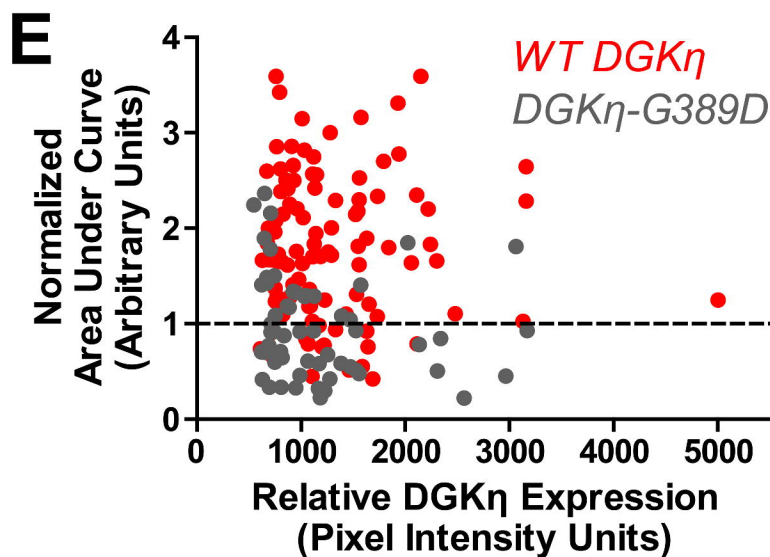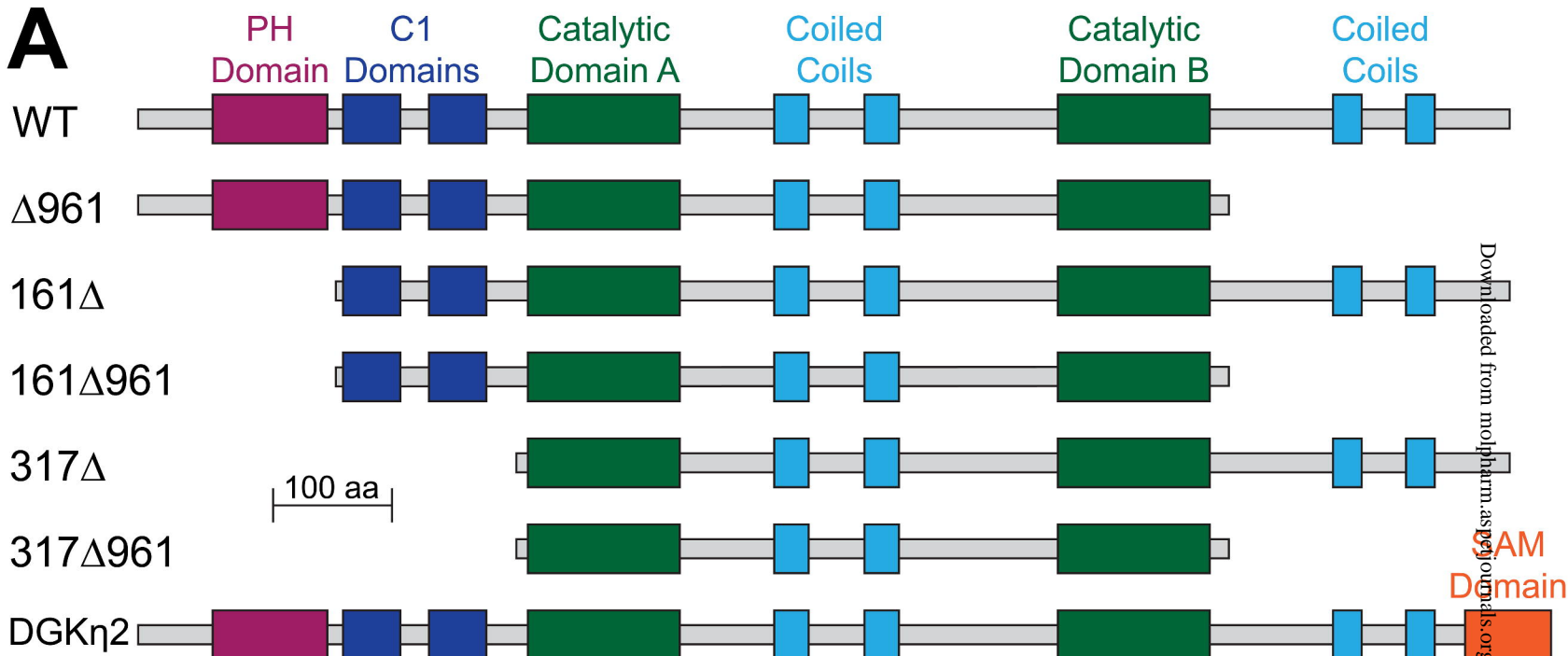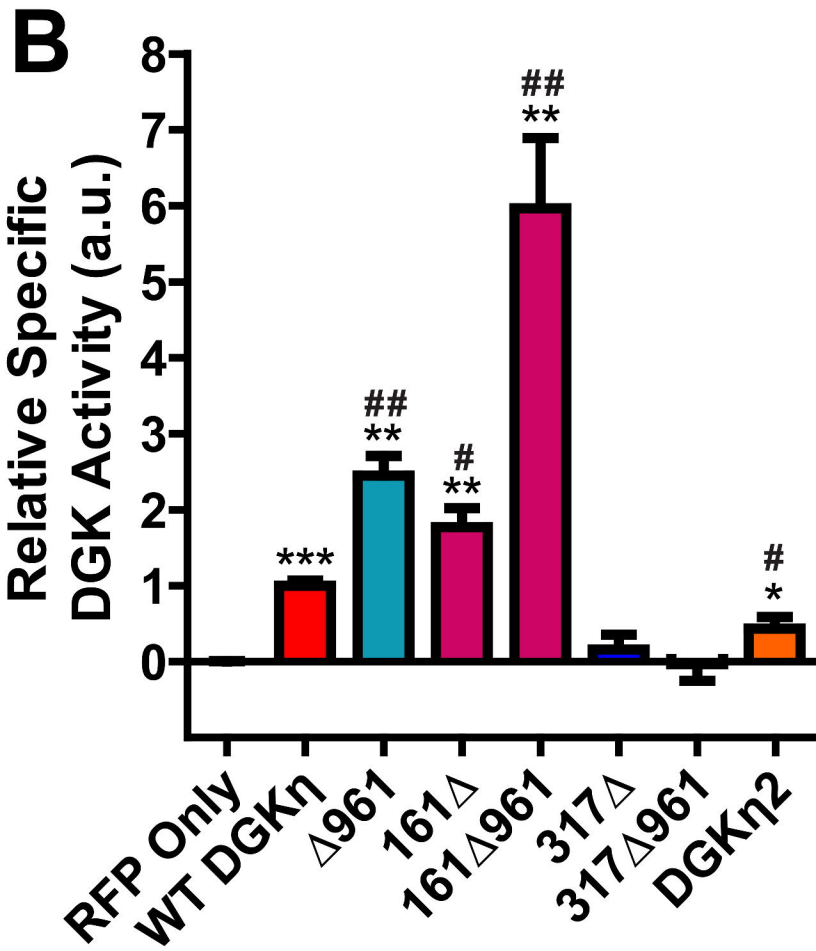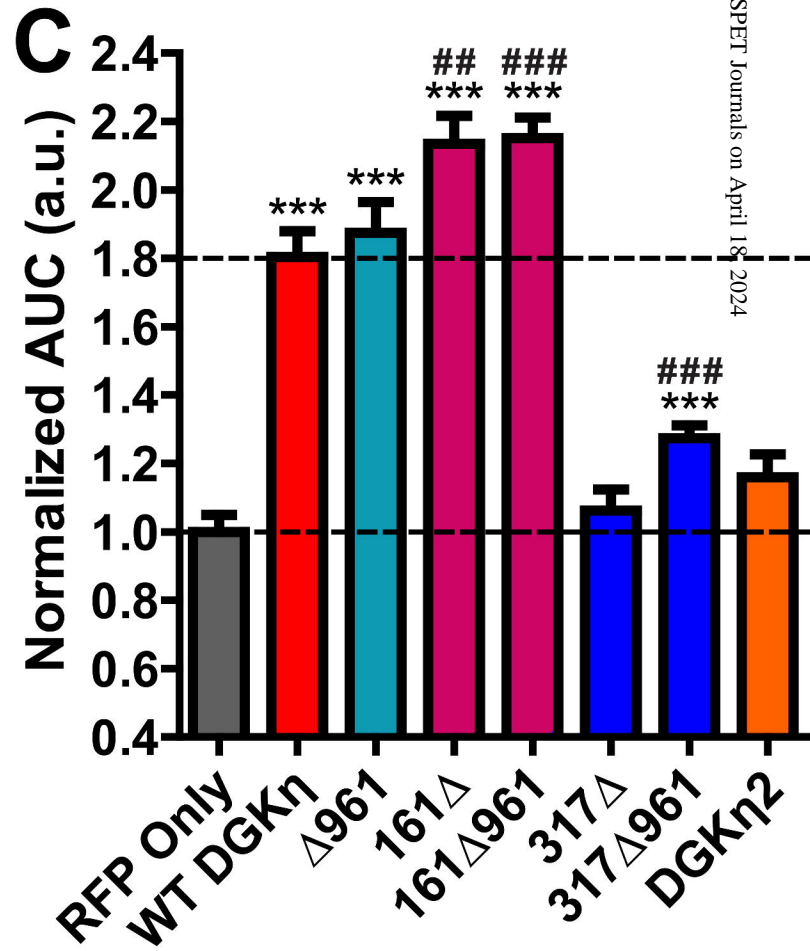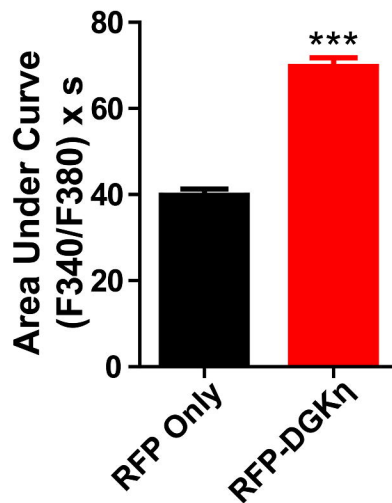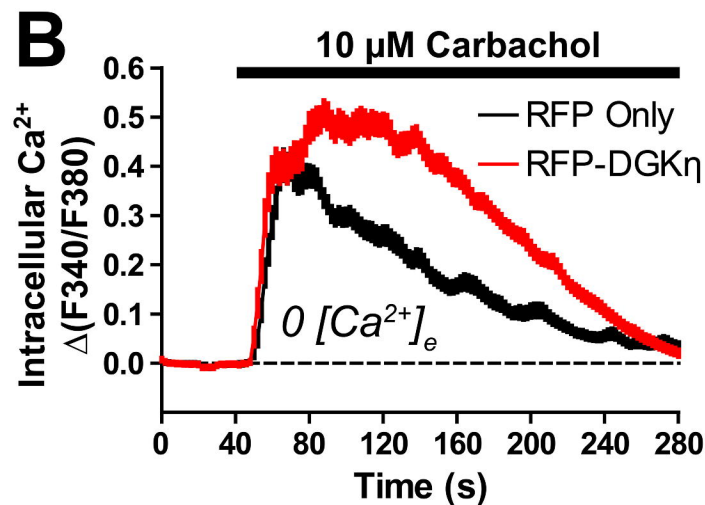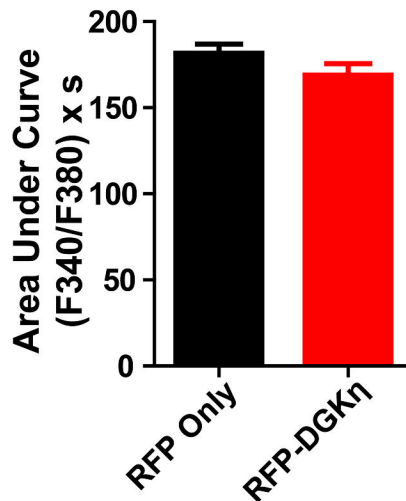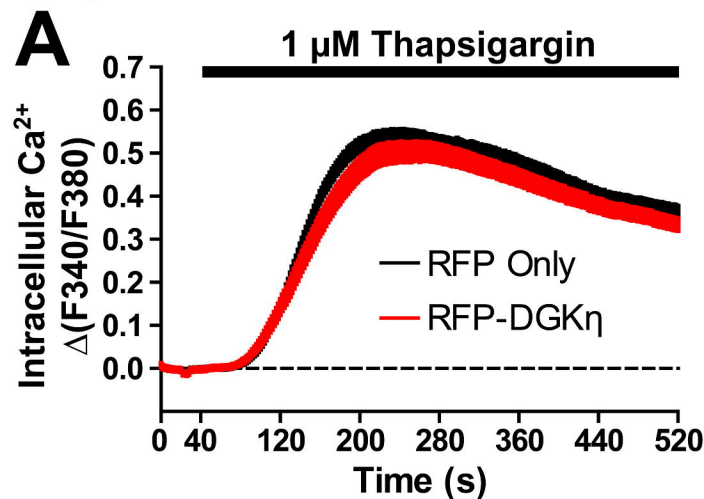
10 µM Carbachol

T = 0' T = 1' T = 5' T = 10' T = 15'
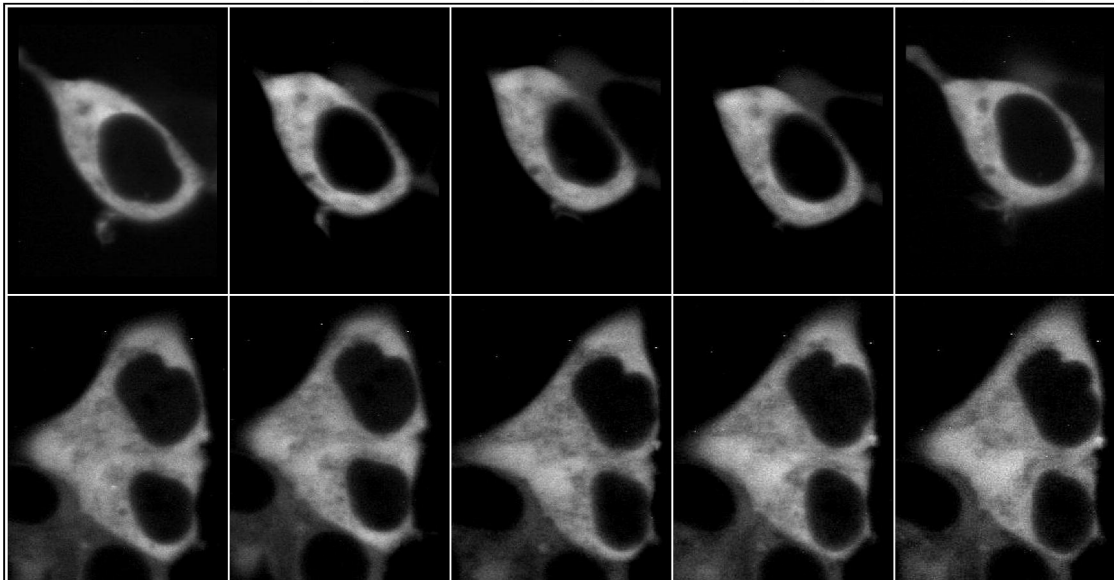
B

500 mM Sorbitol

T = 0' T = 1' T = 5' T = 10' T = 15'

Figure 6

A

Figure 7

A

B